Artificial Neural Network-Based Modeling for Prediction of Hardness of Austempered Ductile Iron

Ravindra V. Savangouder[1](✉), Jagdish C. Patra[1], and Cédric Bornand[2]

[1] Swinburne University of Technology, Melbourne, Australia
rsavangouder@swin.edu.au
[2] University of Applied Sciences HES-SO, HEIG-VD, Yverdon-les-Bains, Switzerland

Abstract. Austempered ductile iron (ADI), because of its attractive properties, for example, high tensile strength along with good ductility is widely used in automotive industries. Such properties of ADI primarily depend on two factors: addition of a delicate proportion of several chemical compositions during the production of ductile cast iron and an isothermal heat treatment process, called austempering process. The chemical compositions, depending on the austempering temperature and its time duration, interact in a complex manner that influences the microstructure of ADI, and determines its hardness and ductility. Vickers hardness number (VHN) is commonly used as a measure of the hardness of a material. In this paper, an artificial neural network (ANN)-based modeling technique is proposed to predict the VHN of ADI by taking experimental data from literature. Extensive simulations showed that the ANN-based model can predict the VHN with a maximum mean absolute error (MAPE) of 0.22%, considering seven chemical compositions, in contrast to 0.71% reported in the recent paper considering only two chemical compositions.

Keywords: Austempered ductile iron · Artificial neural network · Modeling · Prediction · Vickers hardness number

1 Introduction

Austempered ductile iron (ADI), sparked a lot of interest among design engineers due to its high tensile strength with high fatigue strength, good wear resistance and ductility [1]. These desirable properties in ADI are achieved as a result of addition of a delicate proportion of several chemicals (alloying elements) in the ductile iron, and an isothermal heat treatment process called austempering. Since the hardness and ductility in cast-iron are inversely related, its strength and ductility, as desired for a specific application, can be widely varied by carefully selecting the proportion of chemical compositions and by varying the austempering conditions [2, 3]. Because of these characteristics, ADI is widely used in various engineering applications, e.g., manufacturing, railways, and automobiles. Some of the parts produced with ADI are gears, wheel hubs, crankshafts, connecting rods, earth moving machineries and railroads [4–6].

T. Gedeon et al. (Eds.): ICONIP 2019, CCIS 1143, pp. 405–413, 2019.
https://doi.org/10.1007/978-3-030-36802-9_43

ADI belongs to the family of ductile cast irons whose weight percentage of carbon (*C*) and silicon (*Si*) is relatively high as compared to other alloying elements. Ductile cast iron is obtained by magnesium (*Mg*) treatment immediately prior to pouring casting, which produces spheroidal or nodular graphite in ductile iron [7–9]. In order to enhance austempering heat treatment and to achieve desirable mechanical properties, elements such as copper (*Cu*), nickel (*Ni*), molybdenum (*Mo*), manganese (*Mn*), are usually added to ductile iron [2, 8]. During the austempering process, the chemicals interact in a complex and highly nonlinear manner that influences the microstructure which in turn determines the hardness of the ADI. A non-destructive hardness test of a material is commonly used in industry and research because it provides an easy, reliable and inexpensive method to determine basic properties, such as, hardness. Vickers hardness test is one of such tests in which the Vickers hardness number (VHN) of a material can be determined [10]. Due to the complexity involved in the austempering process, any analytical technique to estimate the number and the proportion of the chemicals as well as the austempering temperature and process duration is currently not available.

Recently, artificial neural networks (ANNs) have evolved as a powerful modeling technique for such complex processes. ANNs have been successfully applied to model complex processes in several fields of science and engineering [11, 12], e.g., in modeling solar cells, fuel cells and photovoltaic arrays [13–18]. There has also been a great interest in the materials science community in ANN-based modeling [19–22]. However, only a few studies of ANNs to predict hardness of ADI have been reported [23, 24]. PourAsiabi et al. [24] have proposed a multilayer perceptron (MLP)-based modeling technique to estimate VHN of ADI with eight specimens. However, they have considered only two (out of seven) chemical components, i.e., *Cu* and *Mo*, in their modeling to estimate the VHN and have reported a mean absolute error (MAPE) of 0.71%. Although a tiny proportion of other chemical elements can contribute significantly towards hardness and tensile strength of ADI [2, 8], they have neglected other elements in their model.

In the present paper, we carried out an in-depth study to predict the VHN in ADI using the experimental data reported in [24]. We proposed three MLP-based modeling schemes to predict VHN by taking two, three and seven chemical compositions in the ADI. The major contribution of this paper is as follows. In Model-1, by carefully selecting the MLP parameters, we could achieve a MAPE of 0.33% that is superior to 0.71% that reported in [24]. In Model-2 we introduced an additional important chemical composition, i.e., *Mg*, and shown that it can achieve a maximum MAPE of 0.27%. Next we considered seven chemical constituents in Model-3 and shown that it can achieve a MAPE of 0.22% in predicting VHN. It is noteworthy that our proposed models can predict the VHN, even beyond the range of the training parameters, accurately.

2 Austempering Process of ADI

The austempering process of the ductile iron is commonly identified as a three-step heat treatment process shown in Fig. 1 [1, 2]. In Step-1 (A-B-C), the casting is heated to and held at austenitizing temperature T_γ (815–925 °C) for approximately 2 h. This step is

carried out to make the structure of the casting fully austenitic (γ). In Step-2 (C-D), rapid cooling (quenching) is performed from austenitizing temperature to austempering temperature T_A (ranging between 260–400 °C). Rapid quenching is required to avoid austenite transformation and formation of pearlite. In Step-3 (D-E), the austempering phase, the casting is held at a constant (isothermal) temperature in a salt bath over a period of 1–2 h. Two reactions take place during this isothermal heating depending on the duration of heating. In the first reaction, the austenite (γ) decomposes into acicular ferrite (α) and carbon-rich austenite (γ_{HC}). This microstructure is called ausferrite. If the casting is held at the austempering temperature for too long, a second reaction takes place, during which the carbon-rich austenite decomposes further into ferrite (α) and carbide. This second reaction makes the material brittle, which is an undesirable outcome and hence is avoided. The desirable mechanical properties (e.g., tensile strength and ductility) are obtained in ADI after the completion of the first reaction but before the onset of the second reaction. Finally, the casting is air cooled to room temperature T_{Room} (E-F) [2, 3].

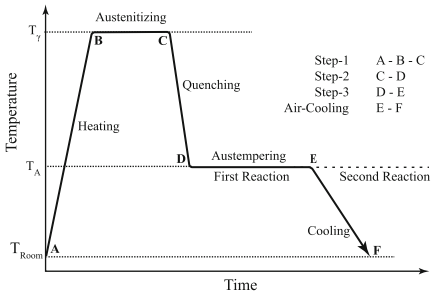

Fig. 1. The ADI austempering process.

3 The ANN and Modeling Scheme

Here, we briefly describe the ANN and the modeling scheme used to predict the VHN of ADI.

3.1 Multilayer Perceptron (MLP)

The MLP is a feed-forward ANN with an input, one or more hidden layers, and one output layer. Each layer contains one or more nonlinear processing units called 'neuron', or 'node'. Each node of a lower layer is connected to all the nodes of an upper layer through links called weights. The backpropagation (BP) algorithm is the most popular learning technique used to train the MLPs [11]. Let Ni, i = 1, 2,…, L, denote the number of nodes in layer i, in which i = 1 denotes the input layer and i = L denotes the output layer. During training process, an input vector, $X = [x_1\ x_2 \ldots\ x_{N1}]$ and a target output vector, $D = [d_1\ d_2 \ldots\ d_{NL}]$, are applied to the MLP. The MLP produces an output vector, $Y = [y_1\ y_2 \ldots\ y_{NL}]$ depending on the weight values of different layers and the nonlinear activation function in each node.

The sum of output square error at the kth instant is given by

$$E(k) = \sum_{i=1}^{N_L} [d_i(k) - y_i(k)]^2 \tag{1}$$

The BP algorithm attempts to minimize the cost function $E(k)$ recursively by updating the weights of the network. The learning and the momentum rates used in the BP algorithm are denoted by α and β, respectively, and their values lie between 0 and 1.

3.2 The ANN-Based Modeling Scheme

Schematic diagrams of the ANN-based modeling of the ADI process are shown in Fig. 2, as a system identification process. Based on the number of chemical compositions used, we propose three MLP-based models to predict the VHN. Model-1 is proposed using *Cu* and *Mo* compositions along with austempering temperature and time in order to determine the influence of these compositions on VHN. The purpose of this model, in addition to verifying the effect of Cu and Mo, is to compare its performance with that of [24]. The influence of *Mg*, although a tiny proportion (about 0.05%), is quite significant in determining the microstructure and the mechanical properties of the ductile iron destined for ADI [7–9]. Therefore, in Model-2 we added *Mg* to Model-1 in order to predict VHN at different austempering temperature and time duration. The overall ADI process that affects the ausferrite microstructure, and in turn, its ductility and hardness, finally depends on all the major chemical compositions [2, 8]. Therefore, in order to predict the VHN, in Model-3 we considered additional four major chemical components, i.e., *C*, *Si*, *Mn* and *Ni* to Model-2.

During the training phase, the input pattern along with its corresponding desired VHN value (the measured value) is applied to the MLP-based model. The output of the model is computed after processing the input pattern in the nodes of different layers of the MLP. Thereafter, the model output is compared with the desired output to generate an error. The resulting error is used to update the weights of the model using the BP algorithm. This process is continued until the MSE_{train} settles to a small value. Thereafter, the trained model is tested for prediction of VHN.

4 Experimental Setup and the Dataset

In the current study, we consider eight specimens with different chemical compositions that have undergone the austempering process with different austempering temperatures and time durations. The experimental data are taken from the article by PourAsiabi *et al*. [24]. The chemical compositions of the eight specimens (in wt%) are given in Table 1. The specimens were austenitized and then were rapidly quenched and soaked in a salt bath at 260, 290, or 320 °C for different time durations, i.e., 30, 60, 90 or 120 min. In this way, twelve samples were created from each specimen, giving rise to a total of 96 samples. The VHN was measured for each sample under 10 kg loading. More details of the experimental setup and procedure can be found in [24].

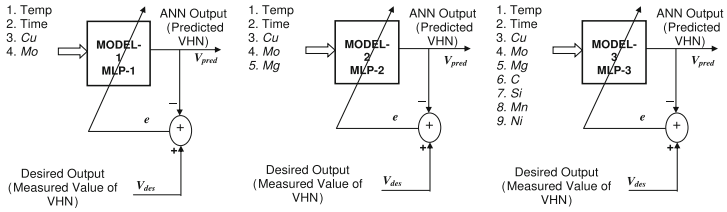

Fig. 2. The three modeling schemes.

Table 1. Chemical Composition of eight specimens in wt%. From PourAsiabi et al. [24].

Chemical composition	Specimen #											
	1	2	3	4	5	6	7	8	Min	Max	Avg.	SD
C	3.44	3.47	3.42	3.42	3.46	3.42	3.45	3.46	3.42	3.47	3.4425	0.0192
Si	2.32	2.35	2.32	2.33	2.41	2.32	2.41	2.42	2.32	2.42	2.3600	0.0424
Mn	0.24	0.24	0.24	0.23	0.25	0.25	0.26	0.26	0.23	0.26	0.2463	0.0099
Ni	1.02	1.01	1.00	1.02	1.00	1.00	1.02	1.02	1.00	1.02	1.0113	0.0093
Cu	0.50	0.50	0.51	0.50	1.00	1.01	1.01	1.00	0.50	1.01	0.7538	0.2513
Mo	0.10	0.15	0.21	0.25	0.10	0.15	0.20	0.25	0.10	0.25	0.1763	0.0566
Mg	0.051	0.052	0.048	0.049	0.053	0.053	0.049	0.054	0.048	0.054	0.0511	0.0021

5 Simulation Setup

All the input variables are normalized between 0 and 1, as per the requirement of the MLP-based modeling. Out of 96 data samples, we used 75% data (72 samples) as training set and the remaining 25% data (24 samples) are used for testing purpose. The learning parameter and momentum factor used in the BP algorithm are gradually decreased with the increase of the iteration, in order to have a faster learning. A bias unit with an output value of +1.0 is added to all layers except the output layer of the MLP. For each model, we carried out several experiments in order to achieve the best architecture and learning parameters. The hidden layer nodes were varied from 5 to 9, and the learning parameters were varied from 0.1 to 0.8. At the end, the best architecture and learning parameters were obtained. The MLP architecture of {5-7-1} in Model-1 implies that it is 3-layer MLP with 5, 7, and 1 node in the input, hidden and output layers (including the bias unit), respectively. Training continued for 10,000 iterations. The MSE at the end of training is found to be lower than −40 dB. This low value of the MLP indicates that the MLP-based models have been well-trained. The architecture of the MLP in Model-2 and Model-3 are given by {6-7-1} and {10-7-1}, respectively. Both the initial learning and momentum rates for the three models are selected as 0.5.

6 Results and Discussion

The scatter plot between the measured and the model estimated VHN values for the complete (96 samples) dataset is shown in Fig. 3a for Model-1. The values of CC, MAPE, and MSE are also shown in this Fig. It can be seen that the CC for both datasets are close to 1.0. In comparison, the CC and MAPE of PourAsiabi *et al.* [24] are 0.9912 and 0.71 respectively. Figure 3b and c shows scatter plots for Model-2 and Model-3 respectively. In Model-2, the CC values for the test set and the complete set are found to be 0.9987 and 0.9992, respectively, thus indicating the effectiveness of modeling. Low values of MAPE indicated high accuracy of estimation of VHN. In Model-3, the CC values for the test set and the complete set are found to be 0.9993 and 0.9995, respectively. The MAPE values for the two sets are found to be 0.33 and 0.22, respectively. These values are superior to the other two models. This is expected, because the VHN is dependent upon the interactions of all the alloying elements during the austempering process. Thus, Model-3 is a complete one that can capture the ADI process accurately.

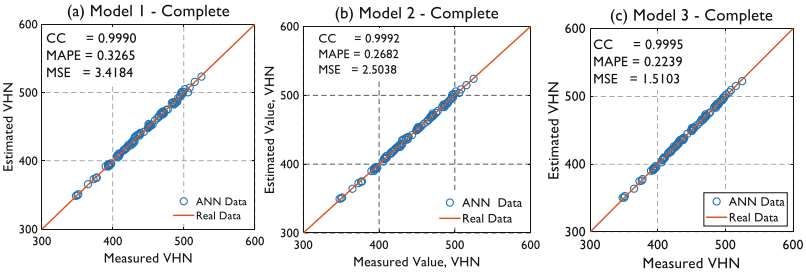

Fig. 3. Scatter plot of measured and estimated VHNs for Model-1, Model-2 and Model-3.

7 Prediction of VHN with MLP Models

Prediction performances of Model-2 at different values of temperature and at four specific austempering time durations, i.e., 30, 60, 90 and 120 min are shown in Fig. 4, for the eight specimens. The red symbols indicate the measured values and the blue symbols denote the predicted values of VHN. It can be seen that the model is able to predict VHN accurately at different values of austempering temperature ranging from 250 to 330 °C. Prediction performances of Model-3 at different values of austempering time duration at three specific austempering temperature, i.e., 260, 290, or 320 °C are shown in Fig. 5, for the eight specimens. The model is able to predict VHN accurately for austempering time duration ranging from 20 to 130 min. This aspect of the MLP-based model has not been reported in [24] or elsewhere.

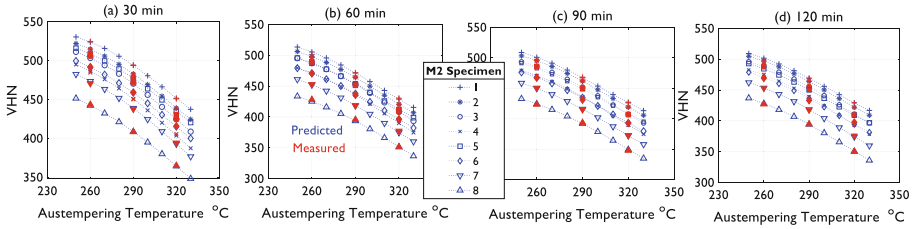

Fig. 4. Model-2 performance. Prediction of VHN at different austempering temperature duration of 30, 60, 90 and 120 min. (Color figure online)

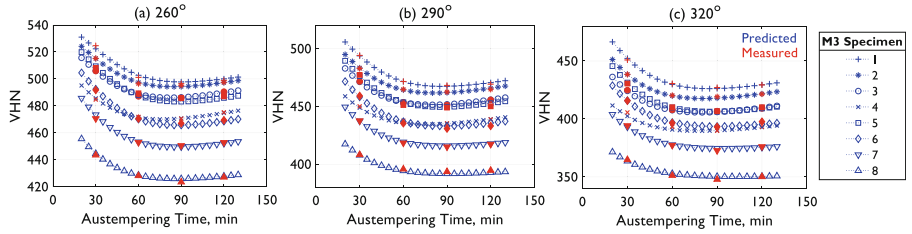

Fig. 5. Model-3 performance. Prediction of VHN at different austempering time duration for austempering temperature of 260, 290 and 320 °C. (Color figure online)

8 Conclusion

We proposed ANN-based techniques for modeling austempering process of ADI to predict VHN. These models can effectively predict VHN at a specific austempering temperature, time duration and, wt% of the seven chemical compositions. We have shown that the correlation coefficient between the measured and estimated VHN values is close to 1.0, thus, indicating high estimation accuracy. The performance of Model-1 is found to be superior to the similar model proposed in [24]. Unlike the other critical chemical constituents that are neglected in [24], the proposed Model-2 and Model-3, respectively, takes three and seven chemical constituents. The mean absolute errors are found to be as low as 0.27% and 0.22% in Model-2 and Model-3, respectively. These models can predict VHN accurately at any value (within a specified range) of austempering temperature and time duration, even beyond the range of training samples. Similar predictions were also achieved for different proportion of chemical compositions (in wt%) at a specific austempering temperature and time duration. One of the major limitations of the current work is the limited amount of available data. Here, we have considered only 96 data samples. However, in a future work, we intend increase dataset by considering other dataset available in the literature. However, these modeling techniques can help in saving time and cost of designing ADI for a specified VHN required for any application.

References

1. Putatunda, S.K.: Development of austempered ductile cast iron (ADI) with simultaneous high yield strength and fracture toughness by a novel two-step austempering process. Mater. Sci. Eng. A **315**, 70–80 (2001)
2. Yazdani, S., Elliott, R.: Influence of molybdenum on austempering behaviour of ductile iron Part 1 – Austempering kinetics and mechanical properties of ductile iron containing 0.13% Mo. Mater. Sci. Technol. **15**, 531–540 (1999)
3. Panneerselvam, S., Martis, C.J., Putatunda, S.K., Boileau, J.M.: An investigation on the stability of austenite in austempered ductile cast iron (ADI). Mater. Sci. Eng. A **626**, 237–246 (2015)
4. C.M.D. Ltd.: Austempered ductile-iron castings — advantages, production, properties and specifications. Mater. Des. **13**, 285–297 (1992)
5. Harding, R.: Austempered ductile irons-gears. Mater. Des. **6**, 177–184 (1985)
6. Cakir, M.C., Bayram, A., Isik, Y., Salar, B.: The effects of austempering temperature and time onto the machinability of austempered ductile iron. Mater. Sci. Eng. A **407**, 147–153 (2005)
7. Angus, H.T.: Cast Iron: Physical and Engineering Properties. Butterworth-Heinemann, Oxford (1978)
8. Trudel, A., Gagne, M.: Effect of composition and heat treatment parameters on the characteristics of austempered ductile irons. Can. Metall. Q. **36**, 289–298 (1997)
9. de Albuquerque Vicente, A., Moreno, J.R.S., de Abreu Santos, T.F., Espinosa, D.C.R., Tenório, J.A.S.: Nucleation and growth of graphite particles in ductile cast iron. J. Alloys Compd. **775**, 1230–1234 (2019)
10. Giannakopoulos, A.E., Larsson, P.L., Vestergaard, R.: Analysis of Vickers indentation. Int. J. Solids Struct. **31**, 2679–2708 (1994)
11. Haykin, S.: Neural Networks. Prentice Hall, Upper Saddle River (1999)
12. Patra, J.C., Kot, A.C.: Nonlinear dynamic system identification using Chebyshev functional link artificial neural networks. IEEE Trans. Syst. Man Cybern. Part B **32**, 505–511 (2002)
13. Patra, J.C.: Neural network-based model for dual-junction solar cells. Prog. Photovoltaics Res. Appl. **19**, 33–44 (2011)
14. Patra, J.C., Chakraborty, G.: e-MLP-based modeling of high-power PEM fuel cell stacks. In: 2011 IEEE International Conference on Systems, Man, and Cybernetics (SMC), Anchorage, AK, pp. 802–807 (2011)
15. Patra, J.C., Maskell, D.L.: Artificial neural network-based model for estimation of EQE of multi-junction solar cells. In: 2011 37th IEEE Photovoltaic Specialists Conference (PVSC), Seattle, WA, pp. 002279–002282 (2011)
16. Patra, J.C.: Chebyshev neural network-based model for dual-junction solar cells. IEEE Trans. Energy Convers. **26**, 132–139 (2011)
17. Jiang, L.L., Maskell, D.L., Patra, J.C.: Chebyshev functional link neural network-based modeling and experimental verification for photovoltaic arrays. In: 2012 International Joint Conference on Neural Networks (IJCNN), Brisbane, QLD, pp. 1–8 (2012)
18. Patra, J.C., Maskell, D.L.: Modeling of multi-junction solar cells for estimation of EQE under influence of charged particles using artificial neural networks. Renew. Energy. **44**, 7–16 (2012)
19. Cool, T., Bhadeshia, H.K.D.H., MacKay, D.J.C.: The yield and ultimate tensile strength of steel welds. Mater. Sci. Eng. A **223**, 186–200 (1997)

20. Malinov, S., Sha, W., McKeown, J.J.: Modeling and correlation between processing parameters and properties in titanium alloys using artificial network. Comput. Mater. Sci. **21**, 375–394 (2001)
21. Yilmaz, M., Ertunc, H.M.: The prediction of mechanical behavior for steel wires and cord materials using neural networks. Mater. Des. **28**, 599–608 (2007)
22. Reddy, N.S., Krishnaiah, J., Young, H.B., Lee, J.S.: Design of medium carbon steels by computational intelligence techniques. Comput. Mater. Sci. **101**, 120–126 (2015)
23. Yescas, M.A.: Prediction of the Vickers hardness in austempered ductile irons using neural networks. Int. J. Cast Met. Res. **15**, 513–521 (2003)
24. PourAsiabi, H., PourAsiabi, H., AmirZadeh, Z., BabaZadeh, M.: Development a multi-layer perceptron artificial neural network model to estimate the Vickers hardness of Mn–Ni–Cu–Mo austempered ductile iron. Mater. Des. **35**, 782–789 (2012)